Inorg. Chem. **2005**, *44*, 4157−4165

Chromium(III) Complexes for Photochemical Nitric Oxide Generation from Coordinated Nitrite: Synthesis and Photochemistry of Macrocyclic Complexes with Pendant Chromophores, *trans*-[Cr(L)(ONO)$_2$]BF$_4$

Frank DeRosa,[1] Xianhui Bu, and Peter C. Ford*

Department of Chemistry and Biochemistry, University of California at Santa Barbara, Santa Barbara, California 93106-9510

Received November 30, 2004

Several new dinitritochromium(III) complexes of the type *trans*-[Cr(L)(ONO)$_2$]BF$_4$, where L is a derivative of the macrocyclic ligand cyclam having pendant aromatic chromophores attached (L = 5,7-dimethyl-6-(substituted)-1,4,8,11-tetraazacyclotetradecane), have been prepared and characterized. Photoexcitation of aqueous solutions containing these complexes at wavelengths corresponding to the pendant chromophore absorption bands led to the generation of NO as detected by an electrochemical sensor. Photophysical data show that the expected fluorescence of the pendant chromophores is largely quenched when the macrocyclic ligand is coordinated to these Cr(III) centers, and this is interpreted in terms of fast energy transfer processes from the ligand-centered $\pi\pi^*$ states to the Cr(III)-centered ligand field states leading to subsequent cleavage of the Cr(III)-coordinated nitrito ligand. Thus, the chromophores tethered to the coordinated cyclam serve as light-gathering antennae for the intramolecular sensitization of the NO-generating photoreactions at the metal center.

Introduction

It is now well-established that nitric oxide (also known as nitrogen monoxide) plays key roles in human cardiovascular and nervous systems and in immune response toward pathogens.[2] These properties have aroused considerable interest in compounds that can be used to deliver NO to biological targets upon demand. Ongoing studies in this laboratory and others have been concerned with the preparation new metal-based compounds having possible applications as photochemically activated drugs to release NO for possible use as a sensitizer in the radiation therapy of tumors.[3−9] For example, this laboratory has reported that aqueous solutions of the complex *trans*-[Cr(cyclam)-(ONO)$_2$]$^+$ (**I**, cyclam = 1,4,8,11-tetraazacyclotetradecane) release NO upon photolysis via the unusual O−N cleavage of the coordinated nitrito ligand with a quantum yield of $\Phi_{NO} = 0.27 \pm 0.03$.[10] However, the low absorption cross section for **I** reduces the potential applicability of this compound as a photochemical NO precursor in living

* Author to whom correspondence should be addressed. E-mail: ford@chem.ucsb.edu.

(1) Taken in part from the Ph.D. dissertation of F.D., University of California, Santa Barbara, CA, 2003.

(2) (a) Palmer, R. M. J.; Ferrige, A. G.; Moncada, S. *Nature* **1987**, *327*, 524−526. (b) Ignarro, L. J.; Buga, G. M.; Wood, K. S.; Byrns, R. E.; Chaudhuri, G. *Proc. Natl. Acad. Sci. U.S.A.* **1987**, *84*, 9265−9269. (c) Hibbs, J. B., Jr.; Taintor, R. R.; Vavrin, Z. *Science* **1987**, *235*, 473−476. (d) Furchgott, R. F.; Vanhoute, P. M. *FASEB J.* **1989**, *3*, 2007−2018. (e) Moncada, S.; Palmer, R. M. J.; Higgs, E. A. *Pharmacol. Rev.* **1991**, *43*, 109−142. (f) Feldman, P. L.; Griffith, O. W.; Stuehr, D. J. *Chem. Eng. News* **1993**, *71*, 10, 26−38. (g) Wink, D. A.; Hanbauer, I.; Grisham, M. B.; Laval, F.; Nims, R. W.; Laval, J.; Cook. J.; Pacelli, R.; Liebmann, J.; Krishna, M.; Ford, P. C.; Mitchell, J. B. *Curr. Top. Cell. Regul.* **1996**, *34*, 159−187. (h) Feelisch, M., Stamler, J. S., Eds. *Methods in Nitric Oxide Research*; John Wiley and Sons: Chichester, England, 1996, and references therein.

(3) Modica-Napolitano, J. S.; Joyal, J. L.; Ara, G.; Oseroff, A. R.; Aprille, J. R. *Cancer Res.* **1990**, *50*, 7876−7881.

(4) (a) Bourassa, J.; DeGraff, W.; Kudo, S.; Wink, D. A.; Mitchell, J. B.; Ford, P. C. *J. Am. Chem. Soc.* **1997**, *119*, 2853−2860. (b) Conrado, C. L.; Wecksler, S.; Egler, C.; Magde, D.; Ford, P. C. *Inorg. Chem.* **2004**, *43*, 5543−5549.

(5) Ford, P. C.; Bourassa, J.; Miranda, K.; Lee, B.; Lorkovic, I.; Boggs, S.; Kudo, S.; Laverman, L *Coord. Chem. Rev.* **1998**, *171*, 185−202.

(6) (a) Lorkovic, I. M.; Miranda, K. M.; Lee, B.; Bernhard, S.; Schoonover, J. R.; Ford, P. C. *J. Am. Chem. Soc.* **1998**, *120*, 11674−11683. (b) Works, C. F.; Ford, P. C., *J. Am. Chem. Soc.* **2000**, *122*, 7592−7593.

(7) Kawakami, M.; Koya, K.; Ukai, T.; Tatsuta, N.; Ikegawa, A.; Ogawa, K.; Shishido, T.; Chen, L. B. *J. Med. Chem.* **1998**, *41*, 130−142.

(8) Mishra, A.; Behera, R. K.; Behera, P. K.; Mishra, B. K.; Behera, G. B. *Chem. Rev.* **2000**, *100*, 1973−2011 and references therein.

(9) (a) Howard-Flanders, P. *Nature (London)* **1957**, *180*, 1191−1192. (b) Mitchell, J. B.; Wink, D. A.; DeGraff, W.; Gamson, J.; Keefer, L. K.; Krishna, M. C. *Cancer Res.* **1993**, *53*, 5845−5848.

(10) (a) DeLeo, M. A.; Ford, P. C *J. Am. Chem. Soc.* **1999**, *121*, 1980−1981. (b) DeLeo, M. A.; Ford, P. C. *Coord. Chem. Rev.* **2000**, *208*, 47−59.

10.1021/ic048311o CCC: $30.25
Published on Web 03/31/2005

Chart 1. Representations of the Dinitritochromium(III) Complex Ions **I**−**V**

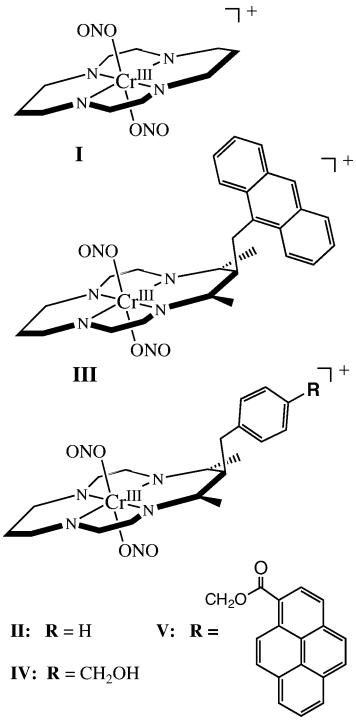

systems. As a consequence, the present research was initiated to prepare compounds having similar features but carrying chromophores that might act as antennas to absorb light more efficiently and as internal sensitizers of the desired photochemistry. Reported here are the syntheses, characterizations, and photochemical properties of several new dinitrito complexes that include aromatic chromophores tethered to modified cyclam-like ligand as illustrated in Chart 1. These compounds provide proof of concept demonstration that pendant chromophores can serve as antennae to gather light and to sensitize excited-state reactions localized at the Cr(III) center leading to the photochemical release of nitric oxide.

Experimental Section

1. Materials and Instrumentation. Silver nitrite, cyclam, dicyclohexylcarbodiimide (DCC), 1-hydroxybenzatriazole, 4-(dimethylamino)pyridine, and 1-pyrenecarboxylic acid were purchased from Aldrich and used without further purification. Dimethylformamide was dried over 3 Å mol sieves before use. We have reported elsewhere the preparations of the ligands mbc (5,7-dimethyl-6-benzylcyclam), mac (5,7-dimethyl-6-anthracylcyclam), and hbc (5,7-dimethyl-6-(*p*-hydroxymethylbenzyl)-1,4,8,11-cyclam) plus their respective dichlorochromium(III) complexes *trans*-[Cr(mbc)Cl_2]Cl, *trans*-[Cr(mac)Cl_2]Cl, and *trans*-[Cr(hbc)Cl_2]Cl.[11]

Electronic spectra were recorded using a Hewlett-Packard model HP8452A diode array spectrophotometer or a Shimadzu model 2401PC spectrophotometer. Low-resolution mass spectra were obtained using a VG Fisons Platform II single quadrupole mass spectrometer with an electrospray ionization source run with a Fisons Masslinks data system. Infrared spectra (KBr pellets) were recorded using an updated BioRad model FTS 60 SPC 3200 FTIR spectrometer. Elemental analyses were carried out by the UCSB Marine Science Institute using a Control Equipment Corp. 440 elemental analyzer.

2. Synthesis of Chromium(III) Dinitrito Complexes. The dinitrito complexes were prepared by the reactions of the dichloro analogues with silver nitrite according to the procedure reported by DeLeo et al.[12] The previously reported[12] *trans*-[Cr(cyclam)-$(ONO)_2$]BF_4 (**I**) was prepared in this manner from *trans*-[Cr(cyclam)Cl_2]Cl with 87.2% yield. ESI-MS (*m*/*z*): 344 (M^+). UV−vis (H_2O) [λ_{max} in nm (ϵ in M^{-1} cm^{-1})]: 336 (271), 476 (33.6). IR (KBr; cm^{-1}): 1493 (ν_{as}, ONO), 987 (ν_s, ONO), 827 (δ_{wag}, ONO).

***trans*-[Cr(mbc)$(ONO)_2$]BF_4 (II).** This was prepared by a procedure adapted from that used to prepare **I**.[12] A solution of *trans*-[Cr(mbc)Cl_2]Cl (0.200 g, 4.19×10^{-4} mol) in H_2O (15 mL) was heated to reflux, and then a hot aqueous solution of $AgNO_2$ (0.194 g, 1.26 mmol) was added under subdued light. A white precipitate (AgCl) formed immediately, and the mixture was refluxed for 45 min during which the solution color turned orange. Upon completion, the mixture was filtered through a medium glass frit and the volatiles were removed from the filtrate under reduced pressure. The orange-brown residue was redissolved in a minimum amount of H_2O (∼3 mL) and passed through a 0.22 μm filter resulting in a deep orange filtrate. The solution was treated with a saturated solution of $NaBF_4$ (10 drops), and the resulting orange precipitate was allowed to settle. Several small scoops of $NaNO_2$ were added, and the solution was sonicated (to ensure dissolution) to salt out the remaining product. The solution was cooled overnight in a refrigerator and then was filtered to give a light orange powder. Yield: 0.210 g (90.9%). ESI-MS (*m*/*z*): 462 (M^+). UV−vis (H_2O) [λ_{max} in nm (ϵ in M^{-1} cm^{-1})]: 328 (271), 472 (31.0). IR (KBr; cm^{-1}): 1496 (ν_{as}, ONO), 982 (ν_s, ONO), 818 (δ_{wag}, ONO). An X-ray crystal structure was obtained.

***trans*-[Cr(mac)$(ONO)_2$]BF_4 (III).** A procedure analogous to one used for the preparation of **II** was employed. Starting with a 0.100 g sample of *trans*-[Cr(mac)Cl_2]Cl (1.73×10^{-4} mol), a yield of 0.033 g (29.2%) was obtained after recrystallization via ether diffusion into a methanol solution of the product to give dark orange crystals. ESI-MS (*m*/*z*) 562 (M^+). UV−vis (H_2O) [λ_{max} in nm (ϵ in M^{-1} cm^{-1})]: 336 (3.94×10^3), 352 (6.55×10^3), 370 (9.29×10^3), 392 (8.47×10^3), 476 (56.0). IR (KBr; cm^{-1}): 1506 (ν_{as}, ONO), 979 (ν_s, ONO), 818 (δ_{wag}, ONO). Anal. Calcd for $CrC_{27}H_{38}N_6O_4BF_4$: C, 49.93; H, 5.89; N, 12.94. Found: C, 50.25; H, 5.58; N, 12.32. An X-ray crystal structure was obtained.

***trans*-[Cr(hbc)$(ONO)_2$]BF_4 (IV).** A procedure analogous to that used for preparation of **II** was employed. Starting with a 0.200 g portion of *trans*-[Cr(hbc)Cl_2]Cl (3.95×10^{-4} mol), a yield of 0.134 g (58.5%) was obtained after recrystallization by ether diffusion into an acetone solution of the product. ESI-MS (*m*/*z*): 492 (M^+). UV−vis (H_2O) [λ_{max} in nm (ϵ in M^{-1} cm^{-1})]: 334 (243), 476 (32.4). IR (KBr; cm^{-1}): 1482 (ν_{as}, ONO), 989 (ν_s, ONO), 823 (δ_{wag}, ONO), 3450 (−OH). Anal. Calcd for $CrC_{20}H_{36}N_6O_5BF_4 \cdot (CH_3)_2C(O)$: C, 43.33; H, 6.64; N, 13.18. Found: C, 43.42; H, 6.37; N, 13.13. An X-ray crystal structure was obtained.

***trans*-[Cr(5,7-dimethyl-6-(1′-methyl-4′-(1″-carboxymethylpyrene)benzyl)-1,4,8,11-tetraazacyclotetradecane)$(ONO)_2$]BF_4, *trans*-[Cr(pbc)$(ONO)_2$]BF_4 (V).** A portion of *trans*-[Cr(hbc)-$(ONO)_2$]BF_4 (0.020 g, 3.45×10^{-5} mol) was dissolved in dry dimethylformamide (10 mL), and to this solution were added 1-pyrenecarboxylic acid (8.5 mg, 3.45×10^{-5} mol), (dimethyl-

(11) DeRosa, F.; Bu, X.; Pohaku, K.; Ford, P. C. Submitted for publication.

(12) DeLeo, M. A.; Bu, X.; Bentow, J.; Ford, P. C. *Inorg. Chim. Acta* **2000**, *300*, 944−950.

amino)pyridine (DMAP) (8.4 mg, 6.90×10^{-5} mol), and hydroxybenzatriazole (HOBt) (5.1 mg, 3.80×10^{-5} mol) at 0 °C in subdued light. The coupling agent dicyclohexylcarbodiimide (DCC) (7.1 mg, 3.45×10^{-5} mol) was added, and the solution was stirred for 1 h at 0 °C. The solution was then warmed to room temperature and stirred for 3 days. The reaction progress monitored by +ESI-TOF mass spectrometry showed an inexplicable nonlinear growth in the peak (*m*/*z* 720), the parent ion *trans*-$[Cr(pbc)(ONO)_2]^+$. There was only modest growth of this peak even at 48 h, but after 72 h, it was dominant in the mass spectrum and the starting material was gone. Upon completion, the solvent was removed under reduced pressure and the resulting dark yellow residue was rinsed with water followed by $CHCl_3$. Yield: 0.016 g (57.6%). ESI-MS (*m*/*z*): 720 (M^+). UV−vis (DMF) [λ_{max} in nm (ϵ in M^{-1} cm^{-1})]: 284 (2.20×10^4), 338 (1.60×10^4), 352 (2.23×10^4), 364 (1.55×10^4), 386 (7.55×10^3), 476 (41.0). IR (KBr; cm^{-1}): 1493 (ν_{as}, ONO), 985 (ν_s, ONO), 820 (δ_{wag}, ONO). Anal. Calcd for $CrC_{37}H_{44}N_6O_6BF_4 \cdot 2CHCl_3$: C, 44.76; H, 4.43; N, 8.03. Found: C, 44.46; H, 4.63; N, 8.37.

3. Crystal Growth and Structure Determination. Crystal structures for compounds **II**−**IV** have been determined. Crystals of **II** and **III** were grown via slow vapor diffusion of ether into a concentrated methanol solution to yield deep orange rectangular crystals. Orange rectangular crystals of **IV** were grown in a similar manner but using acetone in place of methanol.

Suitable crystals were mounted on thin glass fibers with epoxy resin. Low-temperature (150 K) single-crystal studies were carried out on a Bruker Smart 1000 diffractometer equipped with normal-focus 2.4 kW sealed-tube X-ray source (Mo Kα radiation) operating at 50 kV and 40 mA with a two-dimensional CCD detector. The crystals were solved by direct methods followed by difference Fourier methods. Hydrogen atoms attached to carbon atoms were calculated at ideal positions and refined as riding atoms of the parent carbon atoms. The calculations were performed using SHELXTL running on Silicon Graphics Indy 5000. Final full-matrix refinements were against F^2.

4. Photochemical Procedures. Emission and excitation spectra were recorded utilizing a SPEX Fluorolog 2 spectro-fluorometer equipped with a Hamamatsu R928-A water-cooled PMT configured for photon counting and interfaced with a computer running Spex DM3000f software. Emission spectra were corrected for PMT response as well as for lamp intensity variation by the ratio method with a Rhodamine-6G reference. A cutoff filter was placed in front of the emission monochromator to block scattered excitation light. Low-temperature (77 K) emission and excitation data were obtained in a front-face configuration using 4:1 EtOH−MeOH (v/v) glasses. Room-temperature (296 K) emission and excitation data were collected with a right-angle configuration in aqueous media (**I**−**III**) or 1:1 acetonitrile−H_2O (v/v) solvent system (**V**). The more concentrated solutions were 2 mM while diluted samples of **III** and **V** were 50 and 30 μM, respectively. Emission spectra of the free ligands mac and 1-pyrenecroxylic acid were recorded in 50 and 30 μM aqueous solutions, respectively.

Continuous-wave (CW) photolysis experiments were performed in unbuffered aqueous solutions at ambient temperatures with the exception of *trans*-$[Cr(pbc)(ONO)_2]BF_4$ (**V**) that was studied using a 1:1 acetonitrile−H_2O solvent system. Photolysis was performed using a Hg lamp with irradiation wavelengths (λ_{irr}) corresponding to the Hg high-intensity lines at 365 and 436 nm light isolated using interference filters. Ferrioxalate actinometry was used to evaluate light intensities.

Qualitative detection of NO was accomplished using a Harvard Apparatus ami-NO 700 electrochemical NO sensor. The sensor was calibrated using a standard sodium nitrite solution. Care had to be taken not to irradiate the tip of the sensor to avoid a false response. Therefore, the sensor tip was masked within a plastic cell holder, which allowed only a small portion of the quartz cell to be irradiated below the tip by the collimated light. NO-detection experiments were performed in a dark room using 1 cm quartz cells. The cell was filled with 3 mL of deionized water and irradiated using band-pass filters, and small aliquots (30 μL) of aqueous chromium dinitrito solutions were added.

Scheme 1. Synthesis of the Pyrene-Tethered Compound **V**

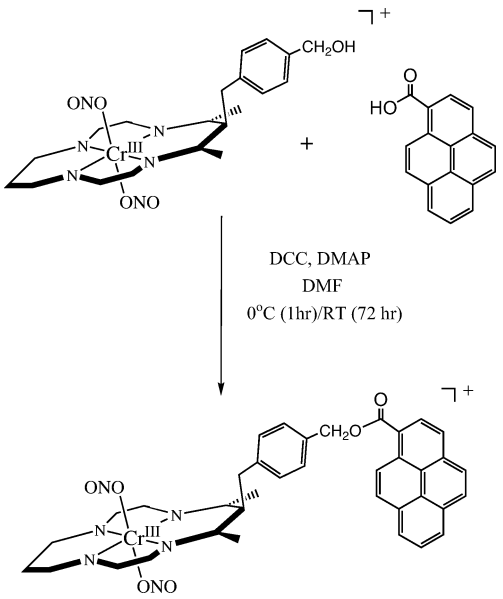

Results and Discussion

1. Syntheses. Reaction of the dichloro complexes *trans*-$[Cr(L)Cl_2]Cl$ (L = mbc, mac, or hbc) with $AgNO_2$ led to formation of the respective dinitrito complexes as reported earlier for **I**.[12] These were recrystallized as BF_4^- salts, and their structures were determined by single-crystal X-ray diffraction methods. The alcohol functionality on the benzyl substituent of *trans*-$[Cr(hbc)(ONO)_2]BF_4$ (**IV**) provides the means to tether additional chromophores to the macrocyclic complex. This was demonstrated using a 1-pyrenecarboxylic acid that was attached via an ester linkage to form *trans*-$[Cr(pbc)(ONO)_2]BF_4$ (**V**) as illustrated by Scheme 1.

2. Spectroscopic Properties. The optical absorption spectra of **II**−**IV** were recorded in aqueous solution. Each displays a quartet to quartet ($Q_1 \leftarrow Q_o$), ligand field (LF) transition at approximately 475 nm (Figure 1, Table 1), derived from the $^4T_{2g} \leftarrow {}^4A_{2g}$ transition expected under octahedral symmetry. Under the roughly D_{4h} symmetry of these complexes, this band would split into $^4B_{2g}$ and $^2E_{2g}$ components, but such splitting is not obvious here. The position of this band is in good agreement with those found for previously characterized chromium(III) nitrito complexes.[12,13] The peak centered at 328 nm ($\epsilon = 271$ M^{-1} cm^{-1}) for **II** and at 334 nm (243 M^{-1} cm^{-1}) for **IV** has been assigned as an intraligand n−π^* transition localized to the coordinated nitrite in analogy to assignments by Fee and

(13) Fee, W. W.; Garner, C. S.; Harrowfield, J. N. B. *Inorg. Chem.* **1967**, *6*, 87−93.

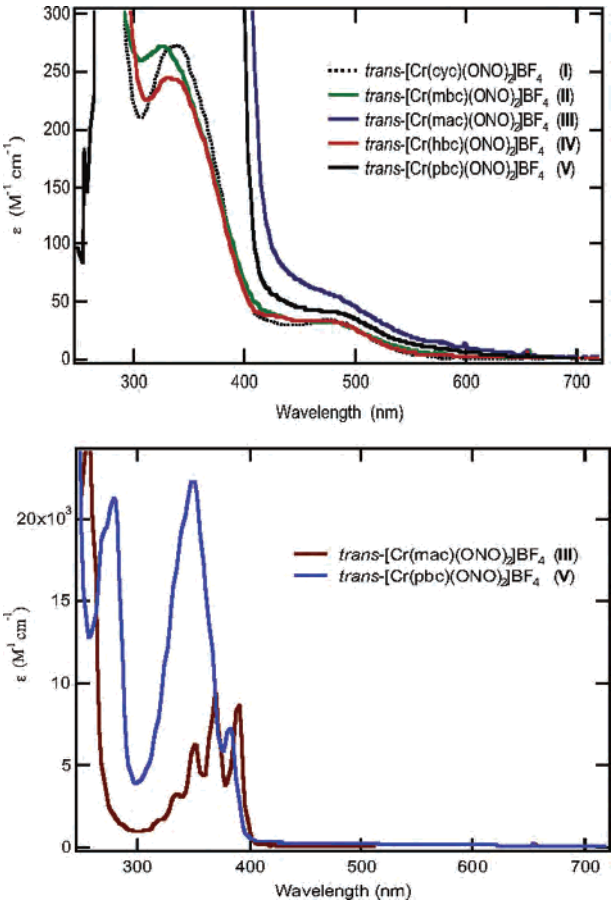

Figure 1. Top: Optical spectra for *trans*-Cr(III) dinitrito complexes **I**−**V**. All spectra are taken in aqueous solutions. Bottom: Absorbance spectra of **III** (50 μM) and **V** (30 μM) in aqueous solution.

Table 1. UV/Vis Spectral Data for Chromium(III) Nitrito Complexes

complex	n−π* λ (nm) (ϵ, $M^{-1}\,cm^{-1}$)	d−d λ (nm) (ϵ, $M^{-1}\,cm^{-1}$)	ref
trans-$[Cr(en)_2(ONO)_2]^+$	328 (185)	477 (44)	13
trans-$[Cr(cyclam)(ONO)_2]^+$ (**I**)	336 (271)	476 (34)	12
trans-$[Cr(tetA)(ONO)_2]^+$	344 (213)	480 (39)	12
trans-$[Cr(mbc)(ONO)_2]^+$ (**II**)	328 (271)	472 (31)	this work
trans-$[Cr(mac)(ONO)_2]^+$ (**III**)	*a*	476 (56)	this work
trans-$[Cr(hbc)(ONO)_2]^+$ (**IV**)	334 (243)	476 (32)	this work
trans-$[Cr(pbc)(ONO)_2]^+$ (**V**)	*a*	476 (41)	this work

[a] n−π* band is masked by π−π* absorption of the aromatic appendage. These bands are listed in the Experimental Section.

Harrowfield[13] for the complex *trans*-$[Cr(en)_2(ONO)_2]ClO_4$. This band tails out to ~400 nm and apparently obscures the higher energy quartet absorptions expected for a D_{4h} Cr(III) diacido tetraamine complex (found at ~370 nm for the dichloro analogues).[11] The ligand-localized n−π* band is obscured in the spectrum of *trans*-$[Cr(mac)(ONO)_2]BF_4$ by the intense π−π* absorption band of the anthracene moiety. Similar absorption bands are seen for the pyrene-derivatized complex, *trans*-$[Cr(pbc)(ONO)_2]BF_4$ (**V**). The quartet to quartet ($Q_1 \leftarrow Q_o$), LF transition appears at 476 nm (41.0 $M^{-1}\,cm^{-1}$), but the n−π* intraligand band is masked by the intense π−π* bands of the pyrene chromophore. For all of these Cr(III) complexes, relatively sharp doublet absorptions ($D_0 \leftarrow Q_o$) are predicted to occur at approximately 650−700 nm;[14] however, these spin-forbidden bands were too weak to be seen in the absorption spectra of these compounds recorded in 5 mM solutions. (Supporting Information Figure S1 displays the absorption spectrum in this region for the parent cylam complex **I**).

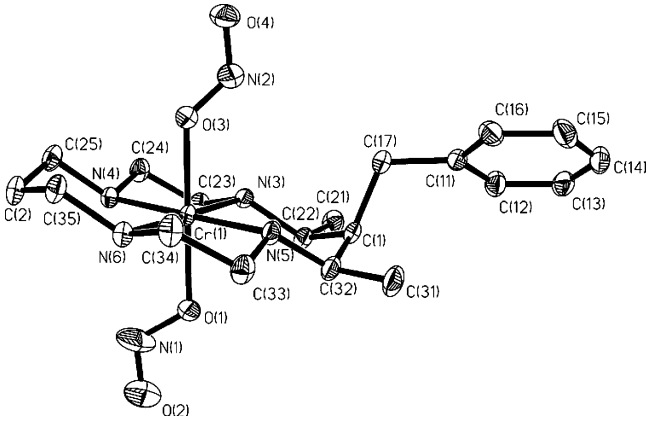

Figure 2. Molecular structure and numbering of atoms for the cation of *trans*-$[Cr(mbc)(ONO)_2]BF_4$ (**II**). Hydrogen atoms are omitted for clarity. Thermal ellipsoids are drawn at the 30% level.

II−**V** were characterized by electrospray ionization time-of-flight (+ESI-TOF) mass spectrometry. In each case, the parent cation (M^+) was seen as well as another, smaller peak 30 *m*/*z* units lower corresponding to the loss of one NO. Similar fragmentation patterns were observed for *trans*-$[Cr(cyclam)(ONO)_2]BF_4$ (**I**).[12]

The FTIR absorbance spectra recorded for **II**−**V** in KBr pellets each displayed three bands characteristic of an O-bound nitrito ligand.[15] For example, *trans*-$[Cr(mbc)(ONO)_2]BF_4$ (**II**) showed bands at 1496 cm^{-1} (ν_{as}, ONO), 982 cm^{-1} (ν_s, ONO), and 818 cm^{-1} (δ_{wag}, ONO) in agreement with previously reported chromium(III) nitrito complexes (Supporting Information, Table S1).[12,13] Each complex also displayed two relatively weak bands representing the N−H wagging modes of trans-configured cyclam ring, for example, at 878 and 892 cm^{-1} for **II**, while the cis isomers would have four bands in this region.[16]

3. Structures. X-ray crystal structures were determined for *trans*-$[Cr(mbc)(ONO)_2]BF_4$ (**II**), *trans*-$[Cr(mac)(ONO)_2]BF_4$ (**III**), and *trans*-$[Cr(hbc)(ONO)_2]BF_4$ (**IV**). The macrocycle resides in the more stable trans-III isoform following nomenclature designated by Bosnich et al.[17] (Figures 2−4). The two methyl groups, C(21) and C(31), are located in equatorial positions while the aryl methyl chromophore is positioned axially on the macrocycle. The higher R_f value for **III** (7.26%) can be attributed to the orientation disorder of the BF_4^- counteranion that persisted even at low temper-

(14) Porter, G. B. In *Concepts of Inorganic Photochemistry*; Adamson, A. W., Fleischauer, P. D., Eds.; John Wiley and Sons: New York, 1975; Chapter 2. Zinato, E. In *Concepts of Inorganic Photochemistry*; Adamson, A. W., Fleischauer, P. D., Eds.; John Wiley and Sons: New York, 1975; Chapter 4.
(15) (a) Nakamoto, K. *Infrared and Raman Spectra of Inorganic and Coordination Compounds*; Wiley: New York, 1986, pp 150 and 224 and references therein. (b) Hitchman, M. A.; Rowbottom, G. L. *Coord. Chem. Rev.* **1982**, *42*, 55.
(16) Poon, C. K.; Pun, K. C. *Inorg. Chem.* **1980**, *19*, 568−569.
(17) Bosnich, B.; Poon, C. K.; Tobe, M. L. *Inorg. Chem.* **1965**, *4*, 1102−1108.

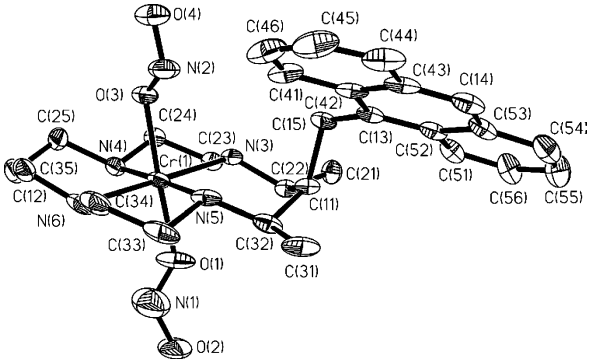

Figure 3. Molecular structure and numbering of atoms for the cation of *trans*-[Cr(mac)(ONO)$_2$]BF$_4$ (**III**). Hydrogen atoms are omitted for clarity. Thermal ellipsoids are drawn at the 30% level.

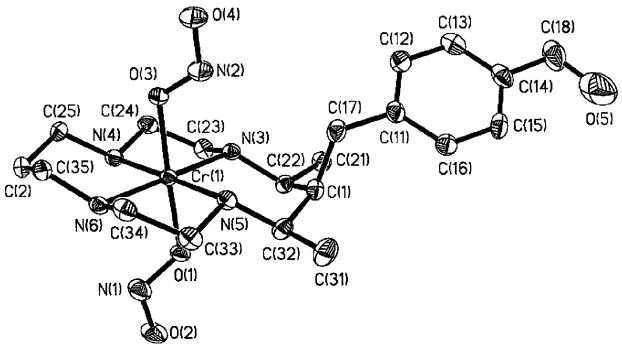

Figure 4. Molecular structure and numbering of atoms for the cation of *trans*-[Cr(hbc)(ONO)$_2$]BF$_4$ (**IV**). Hydrogen atoms are omitted for clarity. Thermal ellipsoids are drawn at the 30% level.

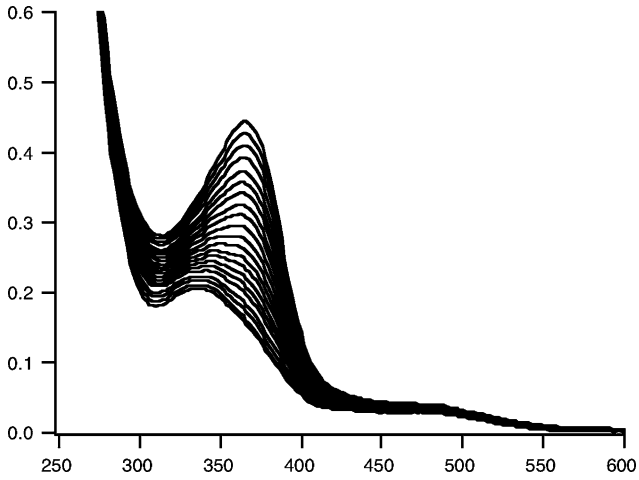

Figure 5. Absorbance increases upon photolysis (λ_{irr} = 365 nm) of an aqueous solution of *trans*-[Cr(mbc)(ONO)$_2$]BF$_4$ (**II**) (1 mM) under aerated conditions at ambient temperature at 1 min intervals for 20 min.

atures (150 K). Selected bond lengths and bond angles are summarized in Tables 2 and 3 and show few differences in key parameters between the four complexes.

4. Continuous Photolysis Studies. ***trans*-[Cr(mbc)(ONO)$_2$]BF$_4$.** The photochemistry of the benzyl derivative **II** is nearly identical with that reported for the unsubstituted complex **I**.[10,18] Aqueous solutions (1 mM) of **II** were photolyzed under aerated conditions at ambient temperature using λ_{irr} = 365 and 436 nm. The qualitative spectral changes were independent of λ_{irr}. Within the first 20 min a new absorption band grew in at 364 nm (ϵ = ~900 M^{-1} cm^{-1}) (Figure 5). The quantum yield was calculated by monitoring these absorption changes at λ_{mon} = 370 nm and plotting the incremental Φ_i versus time. Extrapolation of this plot to the *y*-intercept accounted for inner-filter effects and gave quantum yields of 0.19 ± 0.01 (365 nm) and 0.31 ± 0.03 (436 nm). On the basis of an analogy to the photochemistry of **I**,[10] the product was assigned as the Cr(V) oxo species *trans*-[Cr(mbc)(O)(ONO)]$^{2+}$, formed after the photochemical release of NO and the subsequent oxidation of the putative Cr(IV) primary photoproduct, *trans*-[Cr(mbc)(O)(ONO)]$^{+}$. In deaerated solutions the absorption changes were very small, consistent with DeLeo's demonstration that the primary photoreaction, NO generation from Cr(III)-coordinated nitrite, was rapidly reversible, unless O_2 is present to trap the photochemically generated intermediates (Scheme 2).[10,18]

Continued photolysis (λ_{irr} = 365 nm) of these solutions over much longer time periods (48 h) gave evidence of a secondary photolysis process. Slower spectral changes including a hypsochromic shift to λ_{max} = 356 nm occurred. These slower changes are particularly evident when difference spectra were calculated (Supporting Information Figure S2 top) but did not correspond to the spectrum of a known species. Reinvestigation of the photochemistry of the previ-

Table 2. Selected Bond Lengths (Å) for *trans*-[Cr(mbc)(ONO)$_2$]BF$_4$ (**II**), *trans*-[Cr(mac)(ONO)$_2$]BF$_4$ (**III**), and *trans*-[Cr(hbc)(ONO)$_2$]BF$_4$ (**IV**)

	II	III	IV
Cr(1)−O(1)	1.944(2)	1.946(4)	1.968(2)
Cr(1)−O(3)	1.971(2)	1.968(3)	1.971(2)
Cr(1)−N(3)	2.064(3)	2.073(4)	2.064(3)
Cr(1)−N(4)	2.060(2)	2.058(4)	2.062(3)
Cr(1)−N(5)	2.065(2)	2.065(4)	2.075(3)
Cr(1)−N(6)	2.067(3)	2.065(5)	2.065(3)
N(1)−O(1)	1.296(5)	1.129(8)	1.290(4)
N(1)−O(2)	1.166(4)	1.232(8)	1.209(4)
N(2)−O(3)	1.284(4)	1.239(6)	1.301(4)
N(2)−O(4)	1.206(4)	1.196(5)	1.196(4)

Table 3. Selected Bond Angles (deg) for *trans*-[Cr(mbc)(ONO)$_2$]BF$_4$ (**II**), *trans*-[Cr(mac)(ONO)$_2$]BF$_4$ (**III**), and *trans*-[Cr(hbc)(ONO)$_2$]BF$_4$ (**IV**)

	II	III	IV
O(1)−Cr(1)−O(3)	176.80(10)	175.8(2)	176.97(10)
O(1)−Cr(1)−N(3)	89.22(10)	86.8(2)	86.83(10)
O(3)−Cr(1)−N(3)	93.18(10)	89.3(2)	90.25(10)
O(1)−Cr(1)−N(4)	93.12(10)	90.9(2)	91.20(11)
O(3)−Cr(1)−N(4)	89.17(10)	87.4(2)	87.79(10)
O(1)−Cr(1)−N(5)	87.87(10)	87.6(2)	88.03(11)
O(3)−Cr(1)−N(5)	89.81(10)	94.2(2)	93.00(10)
O(1)−Cr(1)−N(6)	90.73(11)	93.3(2)	93.00(10)
O(3)−Cr(1)−N(6)	86.90(10)	90.6(2)	89.92(10)
N(3)−Cr(1)−N(4)	85.80(10)	86.0(2)	86.08(10)
N(3)−Cr(1)−N(5)	94.96(10)	94.5(2)	94.36(10)
N(3)−Cr(1)−N(6)	179.34(10)	179.5(2)	179.58(11)
N(4)−Cr(1)−N(5)	178.76(10)	178.4(2)	179.09(11)
N(4)−Cr(1)−N(6)	93.55(10)	93.5(2)	86.01(11)
N(1)−O(1)−Cr(1)	121.2(2)	135.6(6)	122.8(2)
N(2)−O(3)−Cr(1)	123.2(2)	121.7(3)	119.4(2)
O(1)−N(1)−O(2)	116.5(4)	122.1(8)	114.8(3)
O(3)−N(2)−O(4)	116.8(3)	118.1(5)	115.4(3)

(18) DeLeo, M. A. Ph.D. Dissertation, University of California, Santa Barbara, CA, 1998.

Scheme 2. Photoreactions of Compound **I** As Outlined by DeLeo[10]

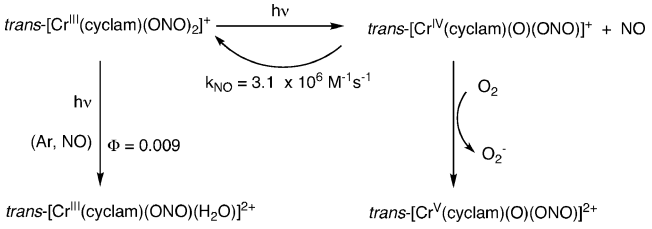

ously studied[10] *trans*-[Cr(cyclam)(ONO)$_2$]BF$_4$ (**I**) in aqueous solutions demonstrated a very similar secondary process (Supporting Information Figure S2 bottom). Quantum yield approximations based upon absorbance changes suggested that the Φ for the second process was about 1 order of magnitude less than that of the first process.

***trans*-[Cr(mac)(ONO)$_2$]BF$_4$.** The strong $\pi-\pi^*$ absorption of the anthracene derivative **III** overlapped other key absorption bands but was only modestly affected by the photochemistry at the Cr(III) center. Photolysis of **III** (50 μM) in an aerated solution with 365 nm light led to small absorption increases in the region where the anthracene $\pi-\pi^*$ bands dominate (Figure 6). The largest differences occurred at 278 nm, and the quantum yield based on absorbance changes at this λ_{mon} was calculated to be 0.17, although a clear assignment of the photochemical processes taking place could not be assessed from these data (see below). When **III** was photolyzed in deaerated aqueous solution (λ_{irr} = 365 nm), changes in the optical spectrum were much smaller ($\Phi < 3.0 \times 10^{-3}$ based on ΔAbs at 278 nm). The latter observation parallels the photochemistry of **I** and **II**, which show only small changes in deaerated solutions owing the reversibility of the NO photolabilization (Scheme 2).

***trans*-[Cr(pbc)(ONO)$_2$]BF$_4$.** Like **III**, continuous photolysis of the pyrene-derivatized complex **V** was carried out at very low concentrations owing to the very strong $\pi-\pi^*$ absorption bands of the pyrene chromophore that dominated the spectrum. An aerated solution of **V** (30 μM) in acetonitrile$-$H$_2$O (1:1 v/v) at ambient temperature was photolyzed (λ_{irr} = 365 nm) under conditions similar to those described for **I**$-$**III**. The changes in the optical spectrum were small owing to the insensitivity of the pyrene group's spectrum (λ_{max} = 352 nm, ϵ = 22 000 M^{-1} cm^{-1}) to changes at the Cr(III) center. However, a $\Delta\epsilon$ value of $\sim$800 M^{-1} cm^{-1} at 314 nm was determined by examining the spectrum after exhaustive photolysis, and from this a quantum yield of $\sim$0.18 was calculated from spectral changes in the initial stages of the photolysis.

Electrochemical NO Detection. Since the spectral changes seen for continuous photolysis experiments were inconclusive with regard to the photochemical processes for **III** and **V**, a NO-specific electrochemical sensor was utilized to monitor the potential photolabilization of NO. For **II** and **III**, aqueous stock solutions (100 μM) were prepared at ambient temperature for these experiments. A cuvette with 3.0 mL of distilled, deionized H$_2$O was placed in front of the photolysis lamp, and the NO-specific electrode was inserted into the cuvette in a manner such that no light was shining on the tip. The solution was irradiated with light from a high-pressure Hg arc lamp using a 360$-$440 nm band-pass filter for wavelength selection. To this solution, a 30 μL aliquot of the Cr(III) stock solution was injected with constant stirring to give a 990 nM concentration of the Cr(III) complex in the photolysis cell. The NO sensor immediately recorded a marked increase in current indicating the formation of free NO in the solution, as expected from the first step of Scheme 2. In contrast, NO was not detected for solutions of the chromium(III) dinitrito complexes in the absence of light.

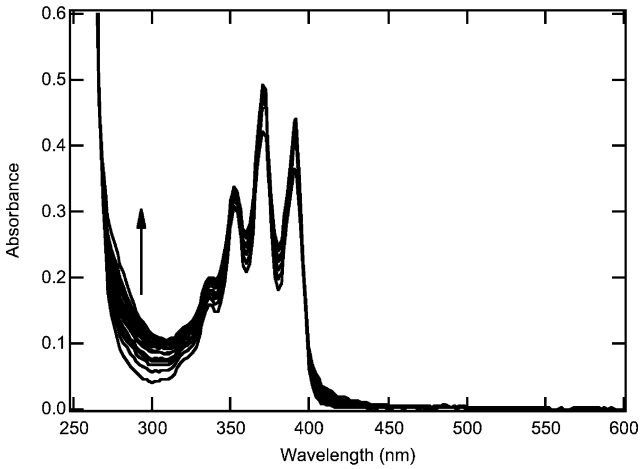

Figure 6. Photolysis of an aqueous solution of *trans*-[Cr(mac)(ONO)$_2$]-BF$_4$ (**III**) (50 μM) under aerated conditions at ambient temperature over a period 20 h. λ_{irr} = 365 nm.

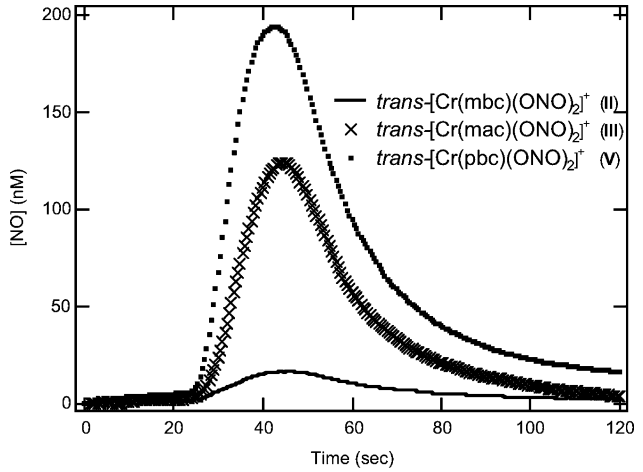

Figure 7. Electrochemical detection of NO upon photolysis of aqueous solutions of **II**, **III**, and **V** irradiating with 360$-$440 nm light (band-pass filter).

These experiments clearly demonstrated that the anthracene derivative *trans*-[Cr(mac)(ONO)$_2$]BF$_4$ produced about *eight* times as much NO (124 nM) as did the benzyl derivative **II** (16 nM) after 20 s photolysis under identical conditions (Figure 7). This difference can be attributed to the much larger absorption cross section at λ_{irr} for **III** at the same concentration. For example, at 365 nm the absorbance of 990 nM **III** is 5.9 $\times$ 10^{-3} while that of 990 nM **II** is $\sim$2 $\times$ 10^{-4}, and **III** would absorb about 30 times as much light as **II** at that wavelength. (However, at the longer wavelengths of the 360$-$440 nm band-pass filter, the

absorbance differences between **II** and **III**, or for that matter between **II** and **V**, are smaller than at 365 nm; see Figure 1.)

Analogous experiments were performed on the pyrene-derivatized analogue **V**. In this case the stock solution was an acetonitrile−H_2O (1:1 v/v) solution of **V** (100 μM) at ambient temperature, and the total concentration after 30 μL aliquot addition was again 990 nM. Photolysis for 20 s using the band-pass filter resulted in NO release (194 nM) (Figure 7) ~60% greater than found for **III** and more than *12 times* that found for **II**. Again, the difference can be attributed to the larger absorption cross section of the pyrene chromophore (0.014 at 365 nm). As noted above, the use of the band-pass filter for excitation makes an accurate calculation of the relative intensity of light absorbed by each of these dilute solutions very difficult. Thus, the correlation between the relative NO signals and the different absorptivities (estimated at 365 nm, but relative differences would be smaller if integrated over the entire excitation range) suggests that the quantum yields for NO loss from these species are comparable. This is consistent with the quantum yield values determined above from changes in the optical spectra. Therefore, the principal differences between these systems in very dilute solutions are the greater absorptivities of **III** and **V** owing to the presence of the light-absorbing antenna tethered to the cyclam ring.

These experiments suggest that photoexcitation of the pendant pyrene and anthracene chromophores is followed by energy transfer to the respective dinitritochromium(III) centers. The efficient NO labilization from the latter demonstrates that the aromatic chromophores can act as antennas for the photosensitization of these systems. Electron transfer from the excited aromatic pendant group to the Cr(III) center would be an alternative mechanism for quenching the fluorescence from these chromophore; however, reduction of the metal center to Cr(II) would lead to nitrite labilization rather than NO release. Since the photochemistry of **III** and **V** parallels that resulting from the direct excitation of the metal-centered ligand field transitions of **I**,[10] we conclude that an energy transfer, rather than excited-state electron-transfer, mechanism is the dominant source of the photochemistry reported here.

Mass Spectral Studies of Photolysis Products. +ESI-TOF mass spectroscopy was used to probe the transformations of the Cr(III) species that accompanied NO photogeneration. For example, 365 nm photolysis of an aqueous solution of **III** (100 μM) was monitored at 10 min intervals over the course of 2 h by taking small aliquots (30 μL) that were then diluted with 100 μL of H_2O and injected into the ESI-TOF instrument. Before photolysis, a large peak at *m*/*z* 562 consistent with the parent cation, *trans*-[Cr(mac)-$(ONO)_2]^+$ (M^+), was present. Over the course of the first 1 h, this peak disappears while new ones at *m*/*z* 533 ($M^+ - 29$) and 504 ($M^+ - 58$) appeared. Over the course of a second 1 h, the peak at *m*/*z* 533 diminished while that at *m*/*z* 504 intensified. No further changes in the mass spectra were observed after the first 2 h for photolysis up to 21 h (Supporting Information Figure S3). The spacing of the photoproduct peaks in this example suggests a sequential process beginning with NO photodissociation in the first step followed by a secondary photoreaction or thermal reaction leading to loss of a second NO. However, such a scenario would requires spacing of these peaks by 30, not 29, *m*/*z* units, unless during the MS analysis process the new Cr(III) oxo species generated are reduced to give mono- and dihydroxyl complexes rather than the oxo or dioxo analogues. This might be expected for high-valent chromium−oxo complexes.[19]

The pattern seen in the photoproduct mass spectral analysis of **III** was also seen for analogous experiments with *trans*-$[Cr(cyclam)(ONO)_2]BF_4$ (**I**) and *trans*-$[Cr(mbc)(ONO)_2]BF_4$ (**II**) done under the same conditions. In general, when the solutions resulting from the photolysis of $[Cr(L)(ONO)_2]^+$ (L = cyclam, mbc, mac) were subjected to mass spectral analysis, the products consistently demonstrate decreased mass from the parent peak (M^+) of *m*/*z* 29 or 58. Since nitric oxide sensor experiments (described above) confirm the direct photochemical release of NO, we conclude that the mass changes of *m*/*z* 29 of the peaks observed upon photolysis of the chromium(III) dinitrito compounds must represent the photochemical loss of NO and with the addition of 1 H^- equiv during the MS experiment.[20]

If one combines the results of the continuous-wave photolysis experiments along with the +ESI-TOF MS experiments and the electrochemical NO detection, it is hypothesized that the growth in absorption seen at 328 nm (species A) after prolonged photolysis of both *trans*-$[Cr(cyclam)(ONO)_2]BF_4$ (**I**) and *trans*-$[Cr(mbc)(ONO)_2]BF_4$ (**II**) is due to the photochemical formation of the Cr(VI) dioxo species *trans*-$[Cr(L)(O)_2]^{2+}$ (where L = cyclam or mbc), perhaps via photochemical NO dissociation (eq 1) from the Cr(V) product *trans*-$[Cr(L)(O)(ONO)]^{2+}$ formed according to processes summarized by Scheme 2.

$$\textit{trans}\text{-}Cr^{V}(L)(O)(ONO)^{2+} \xrightarrow{h\nu} \textit{trans}\text{-}Cr^{VI}(L)(O)_2{}^{2+} + NO \quad (1)$$

5. Photoluminescence Studies. The luminescence spectra of **I**−**IV** were recorded in 77 K (4:1 EtOH−MeOH) glasses at solution concentrations of 2 mM in each case. No phosphorescence from the Cr(III)-centered doublet ligand field state was observed for any of the complexes regardless of the excitation wavelength (355, 370, or 470 nm). This contrasts with the easily observed doublet emission spectra ($\lambda_{em} \sim 704$ nm) for the analogous dichloro complexes *trans*-$[Cr(L)Cl_2]Cl$ under similar conditions. For example, excitation of *trans*-$[Cr(cyclam)Cl_2]Cl$ or *trans*-$[Cr(mbc)Cl_2]Cl$ in low-temperature glasses at 470 nm leads to phosphoresecence,[11,21] but no such emission is seen for quartet LF (470 nm) or n−π^* intraligand (355 nm) excitation of **I** or **II** under analogous conditions. Thus, the latter complexes must

(19) Farrell, R. P.; Lay, P. A. *Commun. Inorg. Chem.* **1992**, *13*, 133−175.
(20) It should be noted that ESR experiments reported only in ref 18 clearly indicated that the photolysis of *trans*-$[Cr(cyclam)(ONO)_2]^+$ (**I**) in aerated aqueous solution leads to the formation of a chromium(V) product *trans*-$[Cr(cyclam)(O)(ONO)]^+$.
(21) Forster, L. S.; Mønsted, O. *J. Phys. Chem.* **1986**, *90*, 5131−5134.

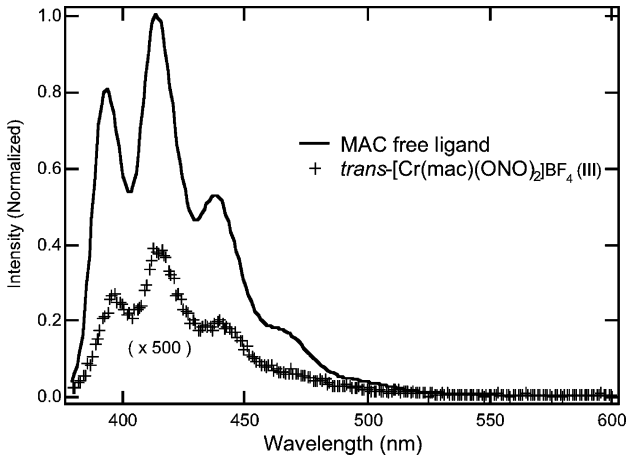

Figure 8. Emission spectra of a dilute aqueous solutions of *trans*-[Cr(mac)(ONO)$_2$]BF$_4$ (**III**) (50 μM) and its respective free ligand, mac (50 μM). λ_{irr} = 360 nm.

undergo efficient excited state deactivation by nonradiative pathways not accessible to the dichloro complexes. Given that chromium(III) dinitrito complexes display fairly large quantum yields for NO release from the coordinated ONO^-,[10] this reaction pathway may be playing a significant role in excited-state deactivation. Since the first step in Scheme 2 is rapidly reversible,[10a] re-formation of the $Cr^{III}-ONO$ entity by the back-reaction of $Cr^{IV}=O$ with NO trapped in the matrix would be fast in low-temperature glasses and net photoreaction might not be detected under these conditions.

The photophysical behavior of the anthracenyl and pyrenyl derivatives *trans*-[Cr(mac)(ONO)$_2$]BF$_4$ (**III**) and *trans*-[Cr(pbc)(ONO)$_2$]BF$_4$ (**V**) are somewhat different. Both display weak luminescence even from dilute ambient-temperature solutions (50 μM in water and 30 μM in (1:1 v:v) acetonitrile$-$H$_2$O, respectively). The weak emission from **III** (λ_{irr} = 360 nm) was characteristic anthracene-type fluorescence with maxima at 397, 414, 440, and 464 nm (Figure 8). The excitation spectrum of this solution (λ_{mon} = 420 nm) displayed peaks at 334, 349, 368, and 386 nm nearly matching the $\pi-\pi^*$ absorption bands of the tethered anthracene (336, 354, 372, and 392 nm, respectively) (Supporting Information Figure S4). A much more intense broad emission centered at 395 nm with a shoulder at 408 nm was observed from the ambient solutions of the pyrene derivative **V** (λ_{irr} = 340 nm). The excitation spectrum displayed an intense, broad band centered at approximately 346 nm with a shoulder at 380 nm similar to the $\pi-\pi^*$ absorption bands of the appended pyrene (352 and 386 nm). Monitoring a solution of **V** for several days showed no changes in the spectroscopic properties; thus, the ester linkage connecting the pyrene carboxylate to the rest of the complex appears to be extremely stable.

The emission and excitation spectra for the free mac ligand (mac = 5,7-dimethyl-6-(9′-methylanthracyl)-1,4,8,11-tetraazacyclotetradecane) (50 mM in aqueous solution) are presented in Figures 8 and S4, respectively. Emission from the free ligand (λ_{irr} = 360 nm) is extremely strong, with bands nearly the same as **III** (394, 414, 438, and 464 nm) but >1000-fold more intense. The excitation spectrum (λ_{mon} = 420 nm) also showed bands (332, 347, 366, and 385 nm) very similar to the $\pi-\pi^*$ absorption spectra (336, 354, 372, and 392 nm, measured in aqueous solution) with an intensity about 3 orders of magnitude larger than that of **III**. Thus, coordination to the dinitritochromium(III) center quenches this emission more than 99.9%, presumably via energy transfer to the states responsible for the photochemical cleavage of the nitrite O$-$N bond and NO formation. A similar situation was observed with the dichloro analogues *trans*-[Cr(mac)Cl$_2$]Cl, namely, weak emission from the anthracene chromophore about 0.1% as intense as that seen for the free ligand under similar conditions.[11] However, as noted above, for the trans-dichloro complex, phosphorescence from the Cr(III) doublet ligand field state was evident, while this was apparently too weak to see for any of the trans-dinitrito analogues.

The emission spectrum of the free chromophore 1-pyrenecarboxylic acid was recorded for comparison to that of **V**. The former displayed a strong emission with a λ_{max} at 394 nm and a shoulder at 408 nm (λ_{irr} = 340 nm), the qualitative aspects of the spectrum being very similar to that observed for **V**. As with the mac ligand, fluorescence from the metal-free 1-pyrenecarboxylic acid chromophore was much stronger than from **V**, although the ratio (~15-fold) was considerably smaller (Supporting Information Figure S5). The excitation spectrum (λ_{mon} = 420 nm) of the former showed a intense, broad peak at 345 nm with a shoulder at 379 nm, shifted slightly from the $\pi-\pi^*$ absorption bands (350 and 384 nm) (Supporting Information Figure S6). This comparison suggests that $\pi\pi^*$ excited states formed by direct excitation of the pyrene chromophore in **V** are deactivated (>90%) by energy transfer to the metal-centered excited states; however, the process may be considerably less efficient than seen with the anthracene derivative **III**. At this stage, we speculate that the lower efficiency of the intramolecular energy-transfer process in **V** can be attributed to the significantly greater distance between the aromatic chromophore and the Cr(III) dinitrito center in **V** than in **III**. From the standpoint of the goals of this paper, it is clear that even in the former case, the overwhelming fraction of the excitation localized on the antenna attached to the macrocyclic cyclam ligand transfers energy to the metal center, thereby sensitizing the photochemical reactions at that site.

In summary, it has been clearly demonstrated that nitric oxide can be photochemically released from these novel chromium(III) dinitrito complexes with high quantum yields. More importantly, it has been shown that such photochemical release can occur via energy transfer from a pendant chromophore to the chromium(III) metal center as demonstrated with the anthracene and pyrene derivatives *trans*-[Cr(mac)(ONO)$_2$]$^+$ and *trans*-[Cr(pbc)(ONO)$_2$]$^+$ resulting in marked increase in the rate of photochemical NO release owing to their greater absorbance at the irradiation wavelengths. These complexes provide proof-of-concept demonstrations that such strategies might be applied to the design of photochemically activated NO donors for biomedical applications.

Acknowledgment. These studies were supported by the U.S. National Science Foundation (Grants CHE 0095144 and CHE-0352650). The mass spectrometry instrumentation (ESI/TOF) was purchased with the support of an ARO award No. DAAD19-00-1-0026. We thank Malcolm DeLeo (Clorox Corp.) and Ryan Absalonson (UCSB) for intellectual and technical input. We also thank Dr. Ziad Taha for his generosity in providing a nitric oxide electrochemical sensor to advance this research.

Supporting Information Available: Listings of complete structure refinement details, bond lengths and angles, anisotropic displacement parameters for non-hydrogen atoms, and hydrogen coordinates and isotropic displacement parameters. This material is available free of charge via the Internet at http://pubs.acs.org.

IC048311O